Symmetry Protected Two-Photon Coherence Time

Xuanying Lai,[1,2,3] Christopher Li,[1,2,3] Alan Zanders,[1] Yefeng Mei,[4,*] and Shengwang Du[1,2,3,†]
[1]*Department of Physics, The University of Texas at Dallas, Richardson, Texas 75080, USA*
[2]*Elmore Family School of Electrical and Computer Engineering, Purdue University, West Lafayette, Indiana 47907, USA*
[3]*Department of Physics and Astronomy, Purdue University, West Lafayette, Indiana 47907, USA*
[4]*Department of Physics and Astronomy, Washington State University, Pullman, Washington 99164, USA*

(Received 30 March 2024; accepted 18 June 2024; published 16 July 2024)

We report the observation of symmetry protected two-photon coherence time of biphotons generated from backward spontaneous four-wave mixing in laser-cooled ^{87}Rb atoms. When biphotons are nondegenerate, nonsymmetric photonic absorption loss results in exponential decay of the temporal waveform of the two-photon joint probability amplitude, leading to shortened coherence time. In contrast, in the case of degenerate biphotons, when both paired photons propagate with the same group velocity and absorption coefficient, the two-photon coherence time, protected by space-time symmetry, remains unaffected by medium absorptive losses. Our experimental results validate these theoretical predictions. This outcome highlights the pivotal role of symmetry in manipulating and controlling photonic quantum states.

DOI: 10.1103/PhysRevLett.133.033601

Entangled photon pairs, termed *biphotons*, generated from spontaneous parametric down-conversion (SPDC) [1–4] or spontaneous four-wave mixing (SFWM) [5–9] have become benchmark tools in quantum optics, particularly for Bell inequality tests [10–13], two-photon interference [14,15], quantum key distribution [16,17], and quantum teleportation [18–20]. Narrow-band biphotons with long coherence times are crucial components for quantum networks [21] due to their efficient interaction with matter nodes, such as atoms and ions. Remarkably, in the absence of significant loss, the two-photon coherence time of biphotons generated in the phase-matching regime is determined by the relative group delay between the paired photons [3,7,22], making it possible to control their temporal characteristics through material dispersion engineering [22].

In open photonic quantum systems, coherence time is typically shortened due to irreversible coupling between the source and the environment, such as loss and dephasing [23,24]. This phenomenon also holds true for biphoton generation when the nonlinear medium (SPDC or SFWM) photon source exhibits absorption. This physics is illustrated in Fig. 1(a). Consider nondegenerate backward biphotons generated within a uniform nonlinear medium of length L. Photon 1 propagates in the $-z$ direction with a slow group velocity $V_g \ll c$ and an absorption coefficient α, while photon 2 moves in the $+z$ direction at the speed of light in vacuum c with no absorption loss. A photon pair can be generated at any point with equal probability within the medium. Two single-photon counters are positioned at both surfaces ($z = 0$ and $z = L$). For two paired photons generated at position z, they arrive at $z = 0$ and $z = L$ with a relative time delay $\tau = t_1 - t_2 \approx z/V_g$. In the absence of loss ($\alpha = 0$), the two-photon coincidence joint probability amplitude appears as a rectangular waveform [dashed line in Fig. 1(a)], with a coherence time of L/V_g, determined by the relative group delay. However, in the presence of absorption ($\alpha > 0$), the field of photon 1 at the output surface $z = 0$ is attenuated to $e^{-\alpha z}\hat{a}_1$, while photon 2 ($\hat{a}_2$) remains unaffected. Consequently, the two-photon coincidence is registered with a relative time delay $\tau = z/V_g$, yielding a two-photon joint probability amplitude

$$\psi(\tau) = \langle 0,0|e^{-\alpha z}\hat{a}_1\hat{a}_2|1,1\rangle \propto e^{-\alpha V_g \tau}, \qquad (1)$$

as depicted by the solid blue curve in Fig. 1(a). When the loss is significant, the resulting two-photon coherence time $1/(2\alpha V_g)$ is significantly shortened compared to L/V_g. This exponential decay waveform is consistent with the results obtained through theory in the interaction picture [7].

Now, let us consider degenerate biphoton generation, where both counterpropagating photons have the same frequency, as shown in Fig. 1(b). They propagate with the same group velocity V_g and the same absorption coefficient α. To count the symmetry, we choose the original position $z = 0$ at the center of the medium. When a photon pair is generated at position z, the field of photon 1, propagating in the $-z$ direction and arriving at $z = -L/2$, becomes $e^{-\alpha(L/2+z)}\hat{a}_1$, while the field of photon 2, propagating in the $+z$ direction and arriving at $z = L/2$, is $e^{-\alpha(L/2-z)}\hat{a}_2$. Thus, the two-photon joint probability amplitude $e^{-\alpha L}$ is independent of position z. As the relative time delay at the

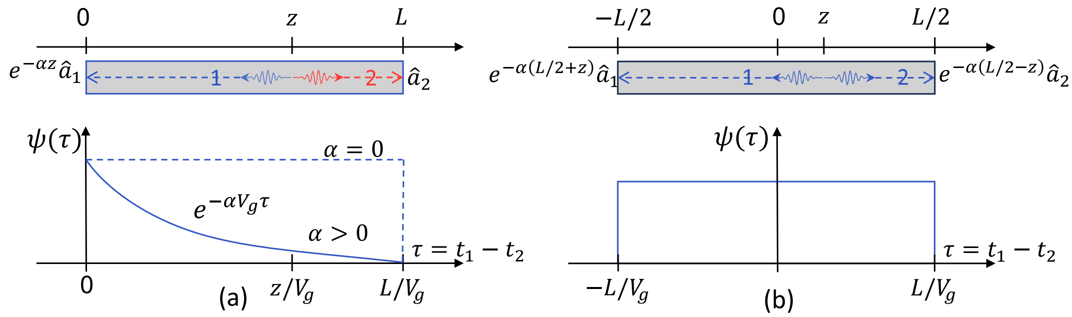

FIG. 1. Biphoton generation in absorptive media. (a) Nondegenerate biphoton generation: photon 1 propagates along the $-z$ direction with a slow group velocity $V_g \ll c$ and an absorption coefficient α, while photon 2 propagates along $+z$ direction with the speed of light in vacuum c and without any absorption loss. (b) Degenerate biphoton generation where both photons 1 and 2 counter propagate with the same slow group velocity V_g and the same absorption coefficient α.

two output surfaces is $\tau = 2z/V_g$, the two-photon joint probability amplitude retains its rectangular shape

$$\psi(\tau) = \langle 0,0|e^{-\alpha L}\hat{a}_1\hat{a}_2|1,1\rangle \propto e^{-\alpha L}\sqcap(\tau; -L/V_g, L/V_g). \quad (2)$$

The rectangular function $\sqcap$, ranging from $\tau = -L/V_g$ to L/V_g, illustrates that the two-photon coherence time is extended to $2L/V_g$. Although the two-photon joint probability amplitude is reduced by a factor of $e^{-\alpha L}$, resulting in a lower coincidence rate, the coherence time of $2L/V_g$ is preserved and protected by symmetry. Unlike the nondegenerate case, symmetry-protected two-photon coherence is independent of photonic absorptive loss.

To experimentally validate the aforementioned predictions, we initially generate nondegenerate narrow-band biphotons from SFWM [7,8,22] in a cloud of ^{87}Rb atoms confined in a two-dimensional (2D) magneto-optical trap (MOT) with a temperature of about 90 μK [25], as illustrated in Fig. 2. The length of the atomic cloud is $L =$ 1.7 cm along its longitudinal z direction. The experiment operates periodically with a cycle duration of 2.5 ms, including a MOT loading and state preparation time of 2.4 ms and a biphoton generation time of 0.1 ms. After the MOT loading time, the atoms are optically pumped to the ground state $|1\rangle$, as depicted in the energy level diagram in Fig. 2(a). The SFWM process is driven by a pair of counterpropagating pump (ω_p, D2 line, 780 nm) and coupling (ω_c, D1 line, 795 nm) laser beams, aligned at an angle of $\theta = 3°$ to the longitudinal z axis, as shown in Fig. 2(b). The circularly (σ^+) polarized pump laser beam with Rabi frequency $\Omega_p = 2\pi \times 3.6$ MHz is blue detuned by $\Delta_p = 2\pi \times 200$ MHz from the transition $|1\rangle \to |4\rangle$. The coupling laser beam (σ^+, $\Omega_c = 2\pi \times 12.2$ MHz) is on resonance with the transition $|2\rangle \to |3\rangle$. Phase-matched backward nondegenerate Stokes (ω_s, 780 nm) and anti-Stokes (ω_{as}, 795 nm) photon pairs are spontaneously produced and collected by a pair of opposing single-mode fibers (SMFs) placed along the MOT longitudinal z axis. We use two narrow-band etalon filters F_1 and F_2 to filter away stray lights. Photon coincidence counts are recorded by two single-photon counting modules (SPCMs). The atomic optical depth (OD) in the anti-Stokes transition is 88 (see Supplemental Material [26] for more detailed experimental parameters). In this nondegenerate case, the anti-Stokes photons propagate with a slow group velocity due to the effect of electromagnetically induced transparency (EIT) [28,29]. The far-off resonance Stokes photons

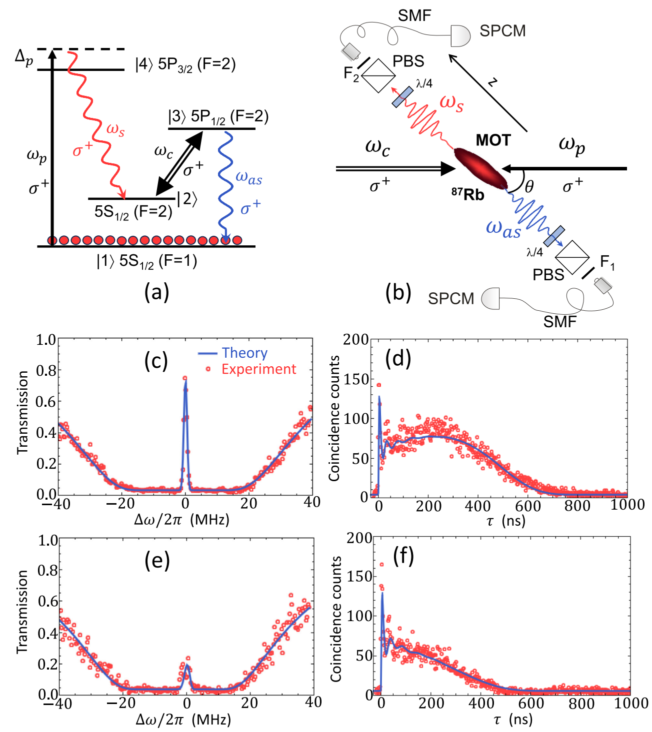

FIG. 2. Nondegenerate biphoton generation via SFWM in cold ^{87}Rb atoms. (a) ^{87}Rb atomic energy level diagram. (b) SFWM optical setup. (c) EIT spectrum with $\alpha L = 0.013$ on resonance. (d) Biphoton coincidence counts under the EIT condition of (c). (e) EIT spectrum with $\alpha L = 0.71$ on resonance. (f) Biphoton coincidence counts under the EIT condition of (e). The coincidence collection time is $T_c = 10$ min. The time binwidth is 2 ns.

propagate at nearly the speed of light in vacuum c with negligible absorption loss.

In our EIT system, the anti-Stokes group delay time can be estimated as $L/V_g \simeq (2\gamma_{13}/|\Omega_c|^2)$OD, and its absorption loss follows $\alpha L = 2\mathrm{OD}\gamma_{12}\gamma_{13}/(|\Omega_c|^2 + 4\gamma_{12}\gamma_{13})$ [7]. Here, γ_{12} is the dephasing rate between the two ground states $|1\rangle$ and $|2\rangle$, and $\gamma_{13} = 2\pi \times 3$ MHz. To keep the group delay time unaffected, we can control the EIT transmission or absorption coefficient by tuning the ground-state dephasing rate γ_{12}. To achieve a small γ_{12}, we switch off the MOT magnetic field during the biphoton generation time and cancel the Earth's residual field with external bias coils. The optimized EIT transmission spectrum is shown in Fig. 2(c). The EIT resonance is nearly transparent with a transmission of 97%, corresponding to a dephasing rate $\gamma_{12} = 2\pi \times 0.0042$ MHz and absorption $\alpha L = 0.013$. The corresponding biphoton correlation $|\psi(\tau)|^2$, measured as two-photon coincidence counts, shown in Fig. 2(d), displays a rectangularlike waveform with a e^{-1} coherence time of 555 ns, consistent with the group delay time obtained from the EIT measurement. The oscillatory peak in the leading edge is the biphoton optical precursor [30,31]. The Gaussian-like tail results from the spatial Gaussian profiles of the pump and coupling laser beams [8,32,33].

Subsequently, we apply an external magnetic field gradient along the z axis to increase the dephasing rate to $\gamma_{12} = 2\pi \times 0.20$ MHz. The resulting EIT transmission spectrum is shown in Fig. 2(e), with the resonance transmission reduced to only 24% ($< e^{-1}$), corresponding to $\alpha L = 0.71$. As predicted, the biphoton correlation displays an exponential decay waveform in Fig. 2(f). The fitted exponential decay time constant is 340 ns, consistent with that obtained from $1/(2\alpha V_g) = 400$ ns with $\alpha = 41.8\ \mathrm{m}^{-1}$ and $V_g = 3.0 \times 10^4$ m/s from the EIT measurement. As expected, the two-photon coherence time is shortened due to nonsymmetric absorption of the paired photons.

We now proceed to experimentally demonstrate degenerate biphotons whose two-photon coherence time is protected by symmetry. As illustrated in Figs. 3(a) and 3(b), the optical setup is nearly identical to that for nondegenerate biphoton generation, but with both pump and coupling lasers now in the ^{87}Rb D1 line (795 nm) (see Supplemental Material [26] for more experimental details). The pump beam is blue detuned from the transition $|1\rangle \to |3\rangle$ by $\Delta_{12} = 2\pi \times 6.8$ GHz, where Δ_{12} is the hyperfine splitting between the two ground levels $|1\rangle$ and $|2\rangle$. The coupling beam is still on resonance to the transition $|2\rangle \to |3\rangle$ with $\Omega_c = 2\pi \times 14.5$ MHz. In this configuration, both spontaneously generated Stokes and anti-Stokes photons are at the same frequency and with the same polarization. Consequently, they experience the same EIT group delay and absorption, fulfilling the symmetry described in Fig. 1(b). The OD for both photons is 150. Similar to the nondegenerate experiment, we vary the medium absorption by tuning the ground-state dephasing rate. Figure 3(c) shows the EIT transmission with small absorption $\alpha L = 0.017$. The corresponding biphoton correlation waveform is displayed in Fig. 3(d). Although there is an oscillatory structure around $\tau = 0$ (biphoton precursor [30,31]) and smoothly turning-off tails at the two ends resulting from the spatial Gaussian profiles of the pump and coupling laser beams [32], the overall waveform exhibits a symmetric rectangularlike shape as expected. We now increase the medium absorption to $\alpha L = 0.85$ and plot the EIT transmission in Fig. 3(e). Unlike the nondegenerate case, the symmetric rectangularlike shape waveform is preserved, though the coincidence counts are reduced due to the larger absorption. The two-photon coherence time of 1250 ns is consistent with the group delay time $2L/V_g = 1350$ ns obtained from the EIT measurements. Thus, we experimentally confirm the symmetry-protected two-photon coherence time in degenerate backward biphoton generation.

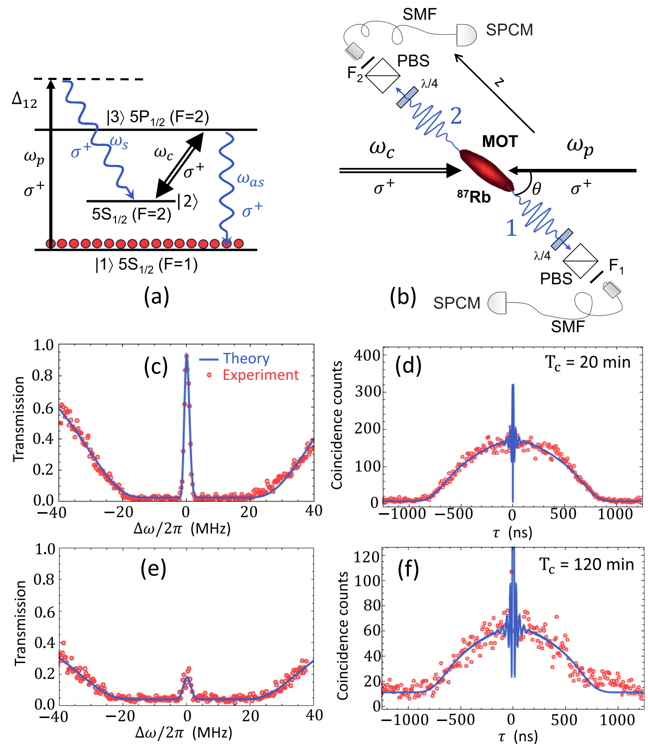

FIG. 3. Degenerate biphoton generation with symmetry protected two-photon coherence. (a) ^{87}Rb atomic energy level diagram. (b) SFWM optical setup. (c) EIT spectrum with $\alpha L = 0.017$ on resonance. (d) Biphoton coincidence counts under the EIT condition of (c) with $\Omega_p = 2\pi \times 218.6$ MHz. (e) EIT spectrum with $\alpha L = 0.85$ on resonance. (f) Biphoton coincidence counts under the EIT condition of (e) with $\Omega_p = 2\pi \times 178.5$ MHz. The time binwidth is 10 ns.

To verify the nonclassical property of the biphoton source, we confirm its violation of the Cauchy-Schwartz inequality [34]. Normalizing the coincidence counts to the accidental background floor in Fig. 3(d), we obtain the normalized cross-correlation function $g_{12}^{(2)}(\tau)$ with a peak value of

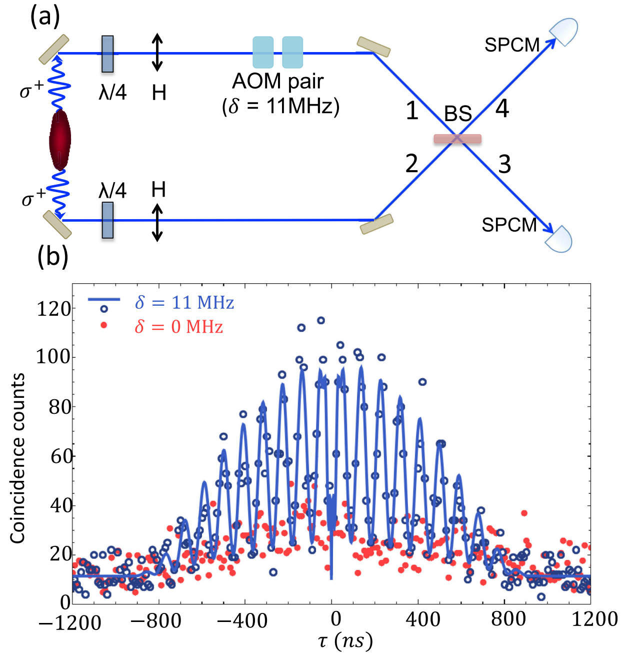

FIG. 4. Biphoton beating experiment. (a) Optical setup. (b) Biphoton beating measured as coincidence counts.

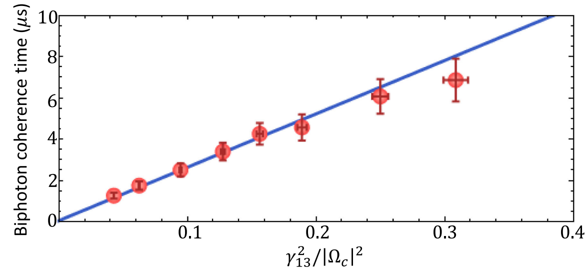

FIG. 5. Biphoton coherence time as a function of $\gamma_{13}^2/|\Omega_c|^2$. The solid line is calculated from $2L/V_g = (4\gamma_{13}/|\Omega_c|^2)\mathrm{OD}$, and the circles are experimental data. OD = 150.

30 ± 11. With the measured autocorrelations $g_{11}^{(2)}(0) = g_{22}^{(2)}(0) = 2 \pm 0.2$, we get $[g_{12}^{(2)}(\tau)]^2_{\max}/[g_{11}^{(2)}(0)g_{22}^{(2)}(0)] = 219 \pm 171$, violating the Cauchy-Schwartz inequality by a factor of 219.

These narrow-band time-energy entangled biphotons can be used to produce heralded single photons with high purity [35], whose conditional autocorrelation function offers another quantitative measure of the quantum nature of the source [36]. Triggered by the detection of photon 1, we pass its paired photon 2 through a beam splitter (BS) whose outputs are connected to two SPCMs. For the biphotons in Fig. 3(d), the measured conditional autocorrelation function is $g_{2|1}^{(2)}(0) = 0.337 \pm 0.069$ with a time window of 1,200 ns, which is below the two-photon threshold value of 0.5.

We further confirm that the symmetry-protected two-photon correlation time preserves their phase coherence by measuring two-photon interference [14,15,27]. The experimental setup for observing two-photon time-resolved interference is depicted in Fig. 4(a). Through the use of quarter-wave ($\lambda/4$) plates, the σ^+ circular polarization of photons 1 and 2 is transformed into horizontal (H) linear polarization. Photon 1 is then subjected to an upper frequency shift of $\delta = 11$ MHz by passing through a pair of acousto-optic modulators (AOMs). Subsequently, both photons are directed into a BS, with their outputs, labeled 3 and 4, detected by two SPCMs. The coincidence pattern, as shown in Fig. 4(b), exhibits a two-photon beating oscillation at a frequency of 11 MHz, with a peak visibility of $78 \pm 4\%$. The deviation from perfect visibility is attributed to the imbalance of the BS, which has a splitting ratio of 30%:70% in our experiment (see Supplemental Material [26]). These findings demonstrate that the correlation time, as measured in Fig. 3(d), indeed corresponds to the phase coherence time of the biphoton joint amplitude.

The EIT group delay time can be estimated as $L/V_g \simeq (2\gamma_{13}/|\Omega_c|^2)\mathrm{OD}$. If absorption loss is not present, we expect the two-photon coherence time to be determined by the group delay time for both nondegenerate and degenerate cases. Therefore, we can increase the two-photon coherence time by reducing the group velocity with a fixed medium length. In a perfect EIT medium with $\gamma_{12} = 0$, this can be achieved by reducing the coupling laser power. However, in a realistic EIT medium with a finite dephasing rate $\gamma_{12} \neq 0$, the absorption loss, $\alpha L \simeq 2\mathrm{OD}\gamma_{12}\gamma_{13}/(|\Omega_c|^2 + 4\gamma_{12}\gamma_{13})$, increases as we reduce the coupling laser power. As a result, for the nondegenerate case, the biphoton coherence time cannot be further increased by reducing the coupling laser power as the absorption loss becomes significant. However, this problem can be overcome in the degenerate case, whose coherence time is protected by symmetry. We confirm this by measuring the two-photon coherence time as a function of $\gamma_{13}^2/|\Omega_c|^2$, as shown in Fig. 5, in which the coherence time increases from 1.25 to 6.85 μs, corresponding to the joint spectral bandwidth from 600 to 80 kHz, by varying the coupling laser power.

The theoretical curves [solid lines in Figs. 2(c)–2(f) and 3(c)–3(f)] are obtained through perturbation theory in the interaction picture [7] (see Supplemental Material [26]). The theory aligns well with the experimental results. In the group delay regime, the biphoton wave function is the Fourier transform of its longitudinal detuning function $\Phi = \mathrm{sinc}(\Delta kL/2)e^{i(k_1+k_2)L/2}$ [7], where $\Delta k \simeq k_1 - k_2 - (k_c - k_p)\cos\theta$ is the complex phase mismatching [9]. Here, $\vec{k}_m$ are the wave vectors of the fields. In the nondegenerate case with significant loss, the longitudinal detuning function can be approximated as $\Phi \simeq i/(\Delta\omega L/V_g + i\alpha L)$ [7], whose Fourier transform gives an exponential decay waveform in Eq. (1). In the degenerate case, the complex EIT wave numbers near resonance are $k_1 \simeq k_0 + \Delta\omega/V_g + i\alpha$ and $k_2 \simeq k_0 - \Delta\omega/V_g + i\alpha$, leading to the cancellation of loss in the phase mismatching $\Delta k \simeq 2\Delta\omega/V_g$. As a result, the longitudinal detuning function becomes

$$\Phi(\Delta\omega) \simeq \mathrm{sinc}\left(\frac{\Delta\omega L}{V_g}\right) e^{-\alpha L}, \tag{3}$$

whose Fourier transform is exactly the biphoton rectangular wave function of Eq. (2). The symmetry cancels losses in the complex phase mismatching, thus protecting the two-photon coherence time.

In summary, we demonstrate symmetry-protected two-photon coherence time in time-frequency entangled biphotons produced via backward SFWM in cold atoms. Contrary to prevailing beliefs that coherence time is reduced by loss and dephasing, our theoretical and experimental findings reveal that space-time symmetry can safeguard the coherence time of entangled photons against loss and dephasing during their generation process. Biphotons with long coherence times are vital for quantum networks due to their efficient interactions with matter nodes such as atoms and ions. Our work introduces a new technique for the manipulation and control of photonic quantum states through symmetry, which play important roles in photonic quantum information processing. Last, we note that the time-space symmetry may also be analyzed using the biphoton Wigner function [37].

The work was supported by DOE (DE-SC0022069), AFOSR (FA9550-22-1-0043), and NSF (2114076, 2228725). Y. M. acknowledges the startup funding from WSU.

*Contact author: yefeng.mei@wsu.edu
†Contact author: du350@purdue.edu

[1] S. E. Harris, M. K. Oshman, and R. L. Byer, Observation of tunable optical parametric fluorescence, Phys. Rev. Lett. **18**, 732 (1967).

[2] D. C. Burnham and D. L. Weinberg, Observation of simultaneity in parametric production of optical photon pairs, Phys. Rev. Lett. **25**, 84 (1970).

[3] M. H. Rubin, D. N. Klyshko, Y. H. Shih, and A. V. Sergienko, Theory of two-photon entanglement in type-II optical parametric down-conversion, Phys. Rev. A **50**, 5122 (1994).

[4] Y. Shih, Entangled biphoton source—Property and preparation, Rep. Prog. Phys. **66**, 1009 (2003).

[5] H. Takesue and K. Inoue, Generation of polarization-entangled photon pairs and violation of Bell's inequality using spontaneous four-wave mixing in a fiber loop, Phys. Rev. A **70**, 031802(R) (2004).

[6] X. Li, J. Chen, P. Voss, J. Sharping, and P. Kumar, All-fiber photon-pair source for quantum communications: Improved generation of correlated photons, Opt. Express **12**, 3737 (2004).

[7] S. Du, J. Wen, and M. H. Rubin, Narrowband biphoton generation near atomic resonance, J. Opt. Soc. Am. B **25**, C98 (2008).

[8] L. Zhao, X. Guo, C. Liu, Y. Sun, M. M. T. Loy, and S. Du, Photon pairs with coherence time exceeding 1 μs, Optica **1**, 84 (2014).

[9] Y. Jiang, Y. Mei, and S. Du, Quantum Langevin theory for two coupled phase-conjugated electromagnetic waves, Phys. Rev. A **107**, 053703 (2023).

[10] S. J. Freedman and J. F. Clauser, Experimental test of local hidden-variable theories, Phys. Rev. Lett. **28**, 938 (1972).

[11] A. Aspect, P. Grangier, and G. Roger, Experimental tests of realistic local theories via Bell's theorem, Phys. Rev. Lett. **47**, 460 (1981).

[12] A. Aspect, J. Dalibard, and G. Roger, Experimental test of Bell's inequalities using time-varying analyzers, Phys. Rev. Lett. **49**, 1804 (1982).

[13] M. Giustina *et al.*, Significant-loophole-free test of Bell's theorem with entangled photons, Phys. Rev. Lett. **115**, 250401 (2015).

[14] C. K. Hong, Z. Y. Ou, and L. Mandel, Measurement of subpicosecond time intervals between two photons by interference, Phys. Rev. Lett. **59**, 2044 (1987).

[15] C. Liu, J. F. Chen, S. Zhang, S. Zhou, Y.-H. Kim, M. M. T. Loy, G. K. L. Wong, and S. Du, Two-photon interferences with degenerate and nondegenerate paired photons, Phys. Rev. A **85**, 021803(R) (2012).

[16] A. K. Ekert, Quantum cryptography based on Bell's theorem, Phys. Rev. Lett. **67**, 661 (1991).

[17] X. Ma, C.-H. F. Fung, and H.-K. Lo, Quantum key distribution with entangled photon sources, Phys. Rev. A **76**, 012307 (2007).

[18] C. H. Bennett, G. Brassard, C. Crépeau, R. Jozsa, A. Peres, and W. K. Wootters, Teleporting an unknown quantum state via dual classical and Einstein-Podolsky-Rosen channels, Phys. Rev. Lett. **70**, 1895 (1993).

[19] D. Boschi, S. Branca, F. De Martini, L. Hardy, and S. Popescu, Experimental realization of teleporting an unknown pure quantum state via dual classical and Einstein-Podolsky-Rosen channels, Phys. Rev. Lett. **80**, 1121 (1998).

[20] D. Bouwmeester, J.-W. Pan, K. Mattle, M. Eibl, H. Weinfurter, and A. Zeilinger, Experimental quantum teleportation, Nature (London) **390**, 575 (1997).

[21] H. J. Kimble, The quantum internet, Nature (London) **453**, 1023 (2008).

[22] S. Du, P. Kolchin, C. Belthangady, G. Y. Yin, and S. E. Harris, Subnatural linewidth biphotons with controllable temporal length, Phys. Rev. Lett. **100**, 183603 (2008).

[23] W. H. Zurek, Decoherence, einselection, and the quantum origins of the classical, Rev. Mod. Phys. **75**, 715 (2003).

[24] M. Schlosshauer, Decoherence, the measurement problem, and interpretations of quantum mechanics, Rev. Mod. Phys. **76**, 1267 (2005).

[25] S. Zhang, J. F. Chen, C. Liu, S. Zhou, M. M. T. Loy, G. K. L. Wong, and S. Du, A dark-line two-dimensional magneto-optical trap of 85Rb atoms with high optical depth, Rev. Sci. Instrum. **83**, 073102 (2012).

[26] See Supplemental Material at http://link.aps.org/supplemental/10.1103/PhysRevLett.133.033601 for more information about the detailed experimental parameters,

theoretical calculation of degenerate biphoton generation, and time-resolved two-photon quantum interference, which include Refs. [7,14,27].

[27] T. Legero, T. Wilk, A. Kuhn, and G. Rempe, Time-resolved two-photon quantum interference, Appl. Phys. B **77**, 797 (2003).

[28] S. E. Harris, Electromagnetically induced transparency, Phys. Today **50**, No. 7, 36 (1997).

[29] M. Fleischhauer, A. Imamoglu, and J. P. Marangos, Electromagnetically induced transparency: Optics in coherent media, Rev. Mod. Phys. **77**, 633 (2005).

[30] S. Du, C. Belthangady, P. Kolchin, G. Y. Yin, and S. E. Harris, Observation of optical precursors at the biphoton level, Opt. Lett. **33**, 2149 (2008).

[31] S. Zhang, J. F. Chen, C. Liu, M. M. T. Loy, G. K. L. Wong, and S. Du, Optical precursor of a single photon, Phys. Rev. Lett. **106**, 243602 (2011).

[32] L. Zhao, X. Guo, Y. Sun, Y. Su, M. M. T. Loy, and S. Du, Shaping the biphoton temporal waveform with spatial light modulation, Phys. Rev. Lett. **115**, 193601 (2015).

[33] L. Zhao, Y. Su, and S. Du, Narrowband biphoton generation in the group delay regime, Phys. Rev. A **93**, 033815 (2016).

[34] J. F. Clauser, Experimental distinction between the quantum and classical field-theoretic predictions for the photoelectric effect, Phys. Rev. D **9**, 853 (1974).

[35] S. Du, Quantum-state purity of heralded single photons produced from frequency-anticorrelated biphotons, Phys. Rev. A **92**, 043836 (2015).

[36] P. Grangier, G. Roger, and A. Aspect, Experimental evidence for a photon anticorrelation effect on a beam splitter: A new light on single-photon interferences, Europhys. Lett. **1**, 173 (1986).

[37] T. Douce, A. Eckstein, S. P. Walborn, A. Z. Khoury, S. Ducci, A. Keller, T. Coudreau, and P. Milman, Direct measurement of the biphoton Wigner function through two-photon interference, Sci. Rep. **3**, 3530 (2013).